Total-Ionizing-Dose Responses of GaN-Based HEMTs With Different Channel Thicknesses and MOSHEMTs With Epitaxial MgCaO as Gate Dielectric

Maruf A. Bhuiyan, *Student Member, IEEE*, Hong Zhou, Sung-Jae Chang, Xiabing Lou, Xian Gong, Rong Jiang, *Student Member, IEEE*, Huiqi Gong, *Student Member, IEEE*, En Xia Zhang, *Senior Member, IEEE*, Chul-Ho Won, Jong-Won Lim, Jung-Hee Lee, *Senior Member, IEEE*, Roy G. Gordon, Robert A. Reed, *Fellow, IEEE*, Daniel M. Fleetwood, *Fellow, IEEE*, Peide Ye, *Fellow, IEEE*, and Tso-Ping Ma, *Fellow, IEEE*

***Abstract*— The radiation hardness of AlGaN/GaN high-electron-mobility transistors (HEMTs) is found to improve with increasing GaN channel thickness. Epitaxial MgCaO shows promise as a radiation-tolerant gate dielectric, with only small shifts in operating parameters of metal–oxide–semiconductor HEMTs observed at doses up to 1 Mrad(SiO_2). Bias-induced electron trapping and radiation-induced-hole trapping can occur in the MgCaO, depending on the applied bias during stress and/or irradiation. AC transconductance measurements are used to help understand charge trapping in these devices.**

***Index Terms*— Atomic layer epitaxy, gallium nitride (GaN) high-electron-mobility transistor (HEMT), metal–oxide–semiconductor HEMT (MOSHEMT), MgCaO, oxide traps, radiation.**

Manuscript received July 14, 2017; revised September 20, 2017, October 27, 2017, and November 8, 2017; accepted November 11, 2017. Date of publication November 17, 2017; date of current version January 17, 2018. This work was supported by DTRA under Contract HDTRA 1-10-1-0042. The work at Harvard University was supported by the Center for the Next Generation of Materials by Design, an Energy Frontier Research Center funded by the U.S. DOE, Office of Science. The work at ETRI and Kyungpook National University was supported in part by ETRI, and in part by the Institute for Information and Communications Technology Promotion funded by Korea Government (MSIP) under Grant 2015-0-00044, and in part by the Semiconductor Industry Collaborative Project between Kyungpook National University and Samsung Electronics Co. Ltd.. The work at Vanderbilt University was supported through the Air Force Office of Sponsored Research under the Hi-REV Program.

M. A. Bhuiyan and T.-P. Ma are with the Electrical Engineering Department, Yale University, New Haven, CT 06511 USA (e-mail: maruf.bhuiyan@yale.edu).

H. Zhou and P. Ye are with the Electrical and Computer Engineering, Purdue University, West Lafayette, IN 47907 USA.

S.-J. Chang and J.-W. Lim are with the Electronics and Telecommunications Research Institute, Daejeon 34129, South Korea.

X. Lou, X. Gong, and R. G. Gordon are with the Department of Chemistry and Chemical Biology, Harvard University, Cambridge, MA 02138 USA.

R. Jiang, H. Gong, E. X. Zhang, R. A. Reed, and D. M. Fleetwood are with the Department of Electrical Engineering and Computer Science, Vanderbilt University, Nashville, TN 37235 USA.

C.-H. Won and J.-H. Lee are with the School of Electronics Engineering, Kyungpook National University, Daegu 702-701, South Korea.

Color versions of one or more of the figures in this paper are available online at http://ieeexplore.ieee.org.

Digital Object Identifier 10.1109/TNS.2017.2774928

I. Introduction

GALLIUM Nitride (GaN) is promising for the next generation power devices for its excellent material properties. Research activities regarding breakdown voltage [1], [2], enhancement mode operation [3], [4], contact resistance [5], [6], surface passivation [7]–[10], etc., have been undertaken to optimize GaN-based power transistor performances. Its wide bandgap, large breakdown electric field, and excellent chemical and thermal stability also make GaN a possible candidate for devices tailored for high-temperature and radiation-intensive environments [11]. The presence of defects in the AlGaN/GaN hetero structure, primarily arising during growth, affects the performance of GaN-based high-electron-mobility transistors (HEMTs) [12]. For example, electrical properties, like mobility and charge trapping, of AlGaN/GaN HEMTs are affected by the presence of threading dislocations in the heterostructure. With increasing GaN channel thickness, threading dislocations arising from lattice mismatches between substrate and GaN layers are more effectively prevented from reaching the upper layers where conduction takes place [12]. Thus, the crystallinity of the heterostructure improves with increasing GaN channel thickness, which in turn improves the electrical performance of as-processed devices. But the effect of channel layer thickness on the total-ionizing-dose (TID) response of AlGaN/GaN HEMTs is not well known.

The quality of the gate dielectric also affects the performance of metal–oxide–semiconductor HEMTs (MOSHEMTs), particularly in terms of gate leakage, subthreshold slope, and ON–OFF current ratio. Recently, GaN-based transistors with extremely high ON–OFF ratios (up to 10^{12}) and low gate leakage have been reported, thanks to the use of atomic layer deposition (ALD) grown epitaxial $Mg_{0.25}Ca_{0.75}O$ as gate dielectric [13], [14]. The performance of earlier-generation GaN HEMTs and MOSHEMTs in a TID has been evaluated,

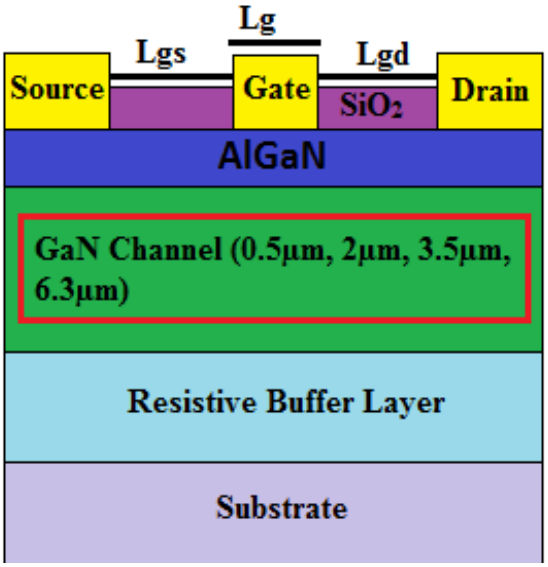

Fig. 1. HEMT structure with various GaN channel thicknesses.

and found to depend on charge trapping in both the AlGaN and oxide layers [15], [16].

In this paper, we evaluate the effects of GaN channel thickness on the TID response of GaN-based HEMTs, and the effects of epitaxial $Mg_{0.25}Ca_{0.75}O$ as a gate dielectric on the TID response of MOSHEMTs. We use ac transconductance measurements to help characterize the trapping in these devices. Both electron and hole trapping can be observed, depending on the bias applied during irradiation. Generally, favorable radiation response is observed in all cases.

II. Devices and Experiments

Wafers for HEMTs and MOSHEMTs were obtained from different sources. The fabrication procedure for $Al_{0.24}Ga_{0.76}N$/GaN HEMTs (Fig. 1) starts with mesa isolation, followed by Ti/Al- and Ni/Au-based source/drain and gate formation, respectively. The access regions (source/gate and gate–drain regions on top of the heterostructure) are passivated with SiO_2. For the HEMT devices, radiation responses of devices with similar dimensions [gate length (L_g) = gate–source length (L_{gs}) = 5 μm, and gate–drain length (L_{gd}) = 10 μm] and various GaN channel thicknesses (0.5, 2, 3.5, and 6.3 μm) have been evaluated. The thickness of the $Al_{0.24}Ga_{0.76}N$ layer is 24 nm.

The fabrication processes for AlGaN/GaN and InAlN/GaN MOSHEMTs (Fig. 2) also start with mesa isolation to an etch depth of 150 nm. Subsequently, ohmic contact formation involves deposition of Ti (15 nm)/Al(60 nm)/Au (50 nm) metal stack, followed by annealing at 775 °C in a nitrogen ambient. Before gate dielectric deposition, the wafers are treated with buffered oxide etch and ammonium hydroxide solution. The oxide stoichiometry is maintained by alternating ALD cycles (one cycle of MgO and three cycles of CaO). The precursors are bis (N, N'-di-*tert*-butylacetamidinato) calcium, bis (N, N'-di-*sec*-butylacetamidinato) magnesium, and water vapour. During oxide growth, the ALD chamber is maintained at 310 °C. The AlGaN MOSHEMT [Fig. 2(a)] consists

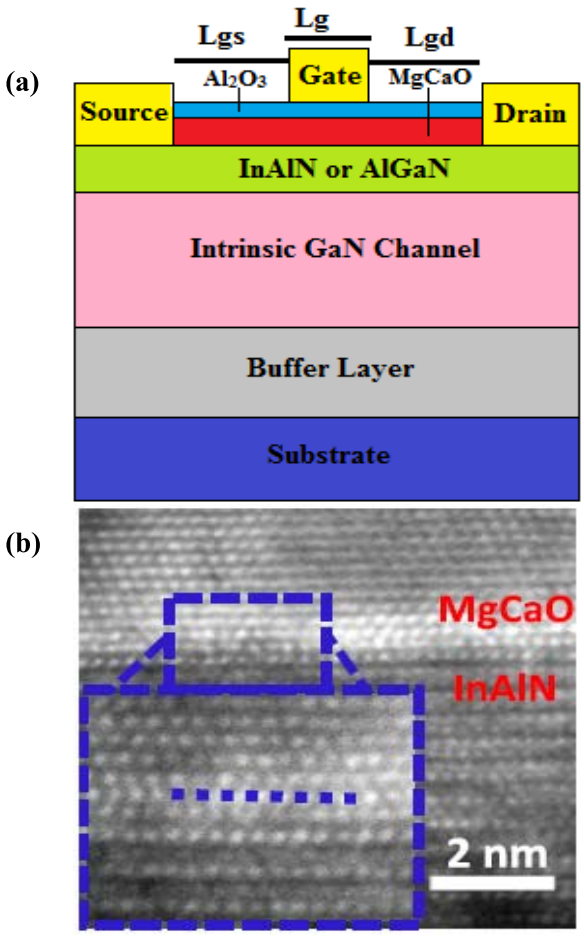

Fig. 2. (a) Schematic of MOSHEMT. (b) TEM image of MgCaO/InAlN interface showing the crystalline quality of the epitaxial oxide [13].

of 8 nm of $Mg_{0.25}Ca_{0.75}O$ capped with 4 nm of Al_2O_3 as gate dielectric, and the InAlN MOSHEMT [Fig. 2(a) and (b)] consists of 4 nm of $Mg_{0.25}Ca_{0.75}O$ capped with 2 nm of Al_2O_3. Thicknesses of the AlGaN and InAlN capping layers are 17 and 6.5 nm, respectively. The intrinsic GaN channel thicknesses for AlGaN and InAlN MOSHEMTs are 600 nm and 1.2 μm, respectively.

For AlGaN MOSHEMTs, the device dimensions are $L_g = 0.8$ μm, $L_{gs} = L_{gd} = 1.1$ μm, and $W = 10$ μm. For InAlN MOSHEMTs, $L_g = 0.12$ μm, $L_{gs} = L_{gd} = 0.7$ μm, and $W = 20$ μm. Devices are irradiated with 10-keV X-rays at a dose rate of 31.5 krad(SiO_2)/min at room temperature, with all terminals grounded, unless otherwise noted.

III. Results and Discussion

A. Impact of GaN Channel Thickness

Fig. 3(a) shows the impact of 10-keV X-ray irradiation on the drain current/gate voltage (I_d–V_g) characteristics of an HEMT device with channel thickness of 0.5 μm. All pins were grounded during irradiation. Electron-hole pairs (EHPs) are created in the structure during irradiation; a fraction are separated by the internal electric field. The generated EHPs may interact with the defects present in the AlGaN layer of the heterostructure during the subsequent carrier-transport

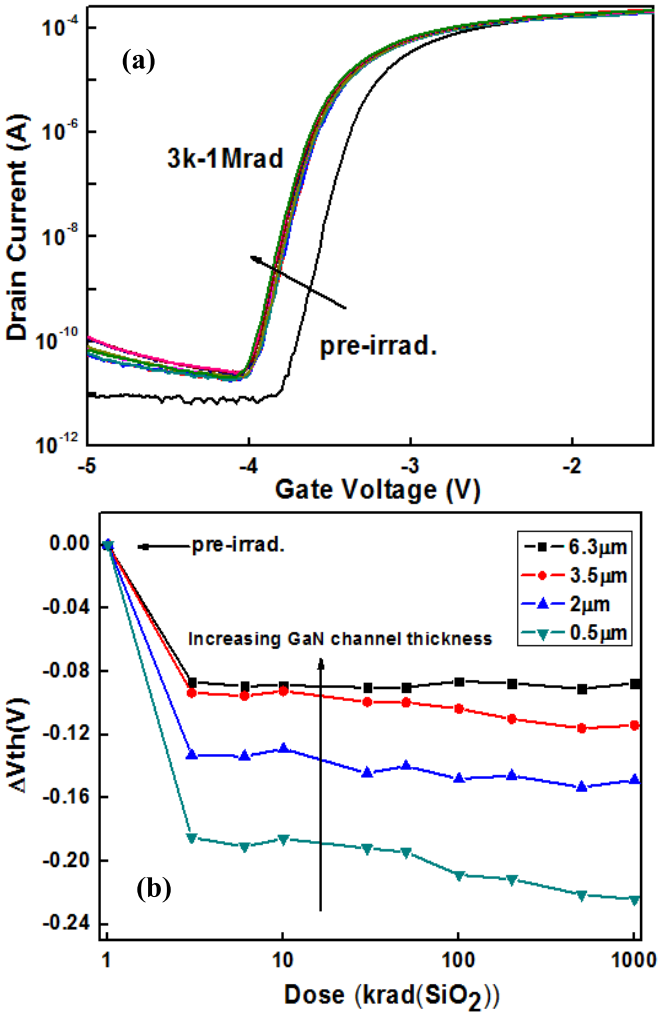

Fig. 3. (a) Effects of 10-keV X-rays on I_d–V_g characteristics, measured with V_{ds} = 50 mV, for a 0.5-μm GaN channel HEMT at doses up to 1 Mrad(SiO_2). (b) V_{th} shifts of HEMTs with four different GaN channel thicknesses for X-ray doses up to 1 Mrad(SiO_2). All terminals are grounded during irradiation.

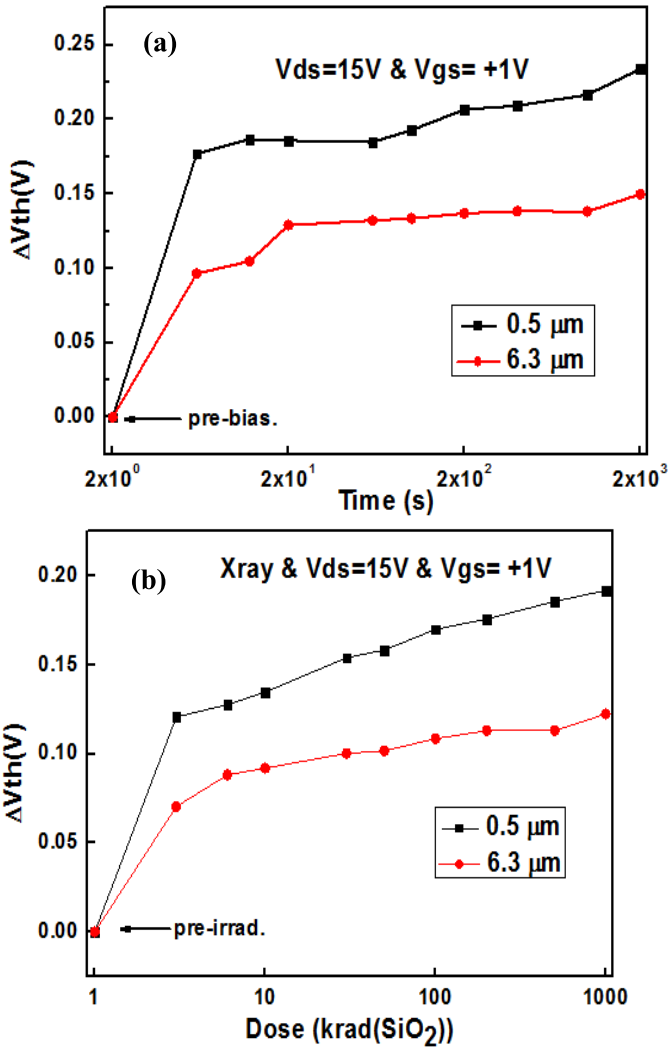

Fig. 4. (a) Effects of bias stress alone. (b) Combined effects of X-ray irradiation and bias stress, on the V_{th} shifts of devices with two different GaN channel thicknesses.

process [15], [17]–[19]. A significant negative shift in the I_d–V_g (drain current versus gate voltage) curve is observed at low doses [~3 krad(SiO_2)].

Fig. 3(b) shows the threshold voltage V_{th} shifts of AlGaN/GaN HEMTs with four GaN channel thicknesses after various X-ray doses. The devices show significant V_{th} shifts for the initial 3 krad(SiO_2) of dose, with smaller changes observed at higher doses. These V_{th} shifts are consistent with the responses of similar GaN-based HEMTs in previous studies, and are attributed to: 1) a shallow energy level for hole traps in the AlGaN layer; 2) neutralization of electron traps that were initially charged in the as-processed devices; and/or 3) the dehydrogenation of defects that were initially passivated with hydrogen [15], [17]–[19]. Any of these three processes can lead to negative shifts in the postirradiation I–V curves, and all are sensitive to the densities of defect precursors in the as-grown devices. It is therefore plausible that a thicker GaN channel leads to reduced V_{th} shifts because the quality of the AlGaN layer is also improved when it is grown on higher quality GaN layer in the thicker channel devices. Hence, the improved postirradiation response is a natural consequence of the reduced defect densities in the as-processed devices.

Next, the impact of bias during radiation is evaluated. Fig. 4(a) shows a significant positive V_{th} shift when devices are biased with 15-V drain-to-source bias (V_{ds}) and 1-V gate-to-source bias (V_{gs}). For both GaN channel thicknesses, electron trapping in the AlGaN layer induced by hot electron injection can explain the observed V_{th} shifts in Fig. 4(a). For the thinner GaN channel, a larger positive shift is observed, which is also consistent with an increased defect density in the AlGaN layer for the thinner channel layer devices. Fig 4(b) shows the V_{th} shifts when the devices are irradiated with similar applied bias. For both GaN channel thicknesses, the observed V_{th} shifts are positive, but smaller than those in Fig. 4(a). This result suggests that radiation-induced holes are captured at bias-induced electron-trapping sites, leading to the partial neutralization of the trapped negative charge in the AlGaN layer, and resulting in a smaller V_{th} shift [18], [19].

TABLE I
PEAK MOBILITY VALUES FOR AlGaN/GaN HEMTs WITH DIFFERENT CHANNEL THICKNESSES

Channel Thickness (μm)	Peak Mobility (cm^2/V.s)	Dislocation Density (10^9 cm^{-2})
0.5	758	7.6
2	1010	1.24
3.5	1190	0.92
6.3	1185	0.87

In addition to improved radiation response, it is also found that the effective peak channel mobility increases with increasing GaN channel thickness, as shown in Table I. Details of the mobility extraction method can be found in [20]. This may be attributed to a reduced amount of Coulomb scattering due to lower density of traps in the AlGaN and/or GaN layers, which is consistent with a reduced as-processed defect density in both device layers [12].

B. $M_{0.25}Ca_{0.75}O$ as Gate Dielectric

Fig. 5 shows I_d–V_g curves for (a) AlGaN and (b) InAlN MOSHEMTs with (a) 4-nm Al_2O_3 and 8-nm MgCaO and (b) 2-nm Al_2O_3 and 4-nm MgCaO as gate dielectric. All pins were grounded during irradiation. Negative V_{th} shifts are observed for all radiation doses, indicating net hole trapping. The initial V_{th} shift at ~3 krad(SiO_2) is similar to the shifts in Fig. 3 for which no oxide is present, and thus likely results from trapping in the heterostructure itself, a conclusion that is consistent also with the results of Sun *et al.* [15]. But in contrast to the saturation of the shift in Fig. 3 at 3 krad(SiO_2), the value of V_{th} continues to increase with dose in Fig. 5. The additional V_{th} shift at higher doses in Fig. 5 is therefore likely to be due to hole trapping in the epitaxially grown $Mg_{0.25}Ca_{0.75}O/Al_2O_3$ gate dielectric. This contrasts with epitaxially grown crystalline La_2O_3 on GaAs substrate, which shows radiation-induced electron trapping [21].

Fig. 6 summarizes (a) the V_{th} shifts and (b) the subthreshold swing (SS) and peak transconductance (G_M) degradation for the devices of Fig. 5. The values of the SS are obtained from the dc I_d–V_g curves in the subthreshold region via the relation $SS = dV_g/d(\log I_d)$ [22]. Values of G_M are calculated from the first derivative of the dc I_d–V_g curves.

The V_{th} shifts for the InAlN MOSHEMTs in Fig. 6(b) are smaller than those of the AlGaN MOSHEMTs in Fig. 6(a) most likely because of the reduced dielectric layer thickness, which naturally leads to reduced radiation-induced-hole trapping in amorphous [23] and epitaxial [21] oxides. Furthermore, InAlN MOSHEMTs have a thinner capping layer than AlGaN MOSHEMTs, which may also contribute to the observed improvement in response. Finally, we note that similar channel thickness effects on TID response also have been observed in germanium on insulator transistors [24].

Fig. 6(b) shows a significant increase in SS for the AlGaN MOSHEMT, but little change in peak transconductance. It is likely that the increase in SS results from radiation-induced border traps and/or charge lateral nonuniformities (LNUs)

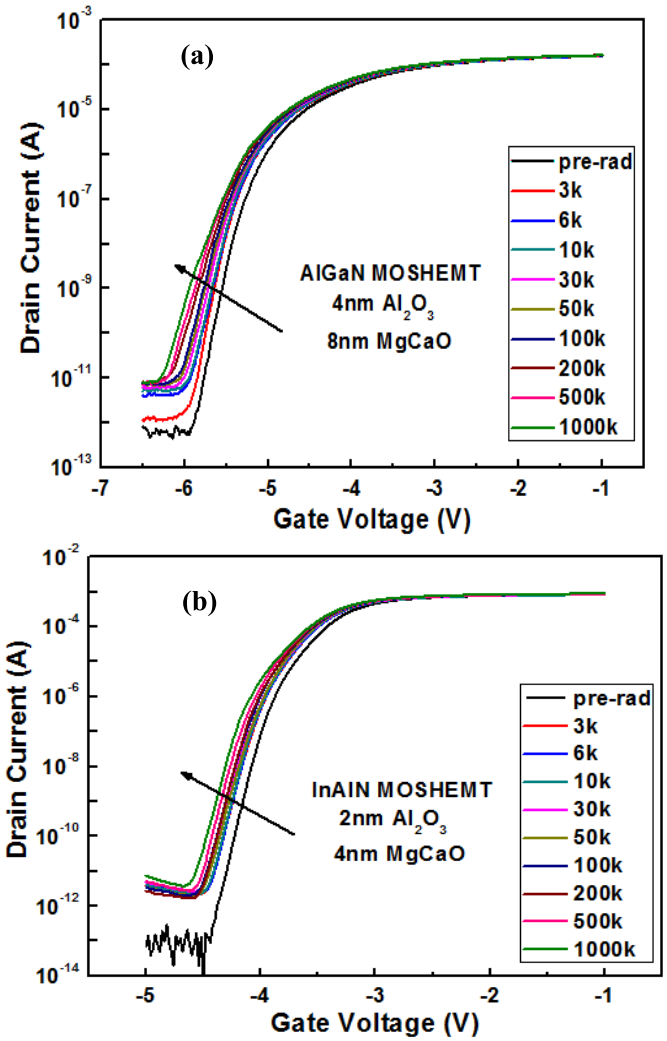

Fig. 5. I_d–V_g curves, measured with V_{ds} = 50 mV, for (a) AlGaN and (b) InAlN MOSHEMTs with (a) 4-nm Al_2O_3 and 8-nm crystalline MgCaO and (b) 2-nm Al_2O_3 and 4-nm crystalline MgCaO as gate dielectric for X-ray irradiation up to 1 Mrad(SiO_2). All terminals are grounded during irradiation.

in the dielectric layer than the buildup of radiation-induced interface traps because each of these types of traps are more easily passivated during TID exposure than are interface traps [23]. Charge LNUs are due to variations in the trapped charge density along the channel; border traps result from slow charge exchange between near-interfacial traps in the dielectric and the carrier channel. These radiation-induced border traps and/or LNUs in the dielectric layer can cause stretchout in the current voltage characteristics without affecting mobility significantly because the trapped charge is more distant from the charge carriers in the channel than are interface traps. Each of these possibilities are similar to what has been observed in Si-based MOS devices subjected to ionizing radiation exposure [25]–[27], as well as in as-processed and irradiated GaN-based HEMTs [17], [18], [28], [29].

C. Bias Dependent Radiation Response of $Mg_{0.25}Ca_{0.75}O$ Gate Dielectric

The effects of bias are evaluated for AlGaN MOSHEMTs with 4-nm Al_2O_3 and 8-nm MgCaO as gate dielectric.

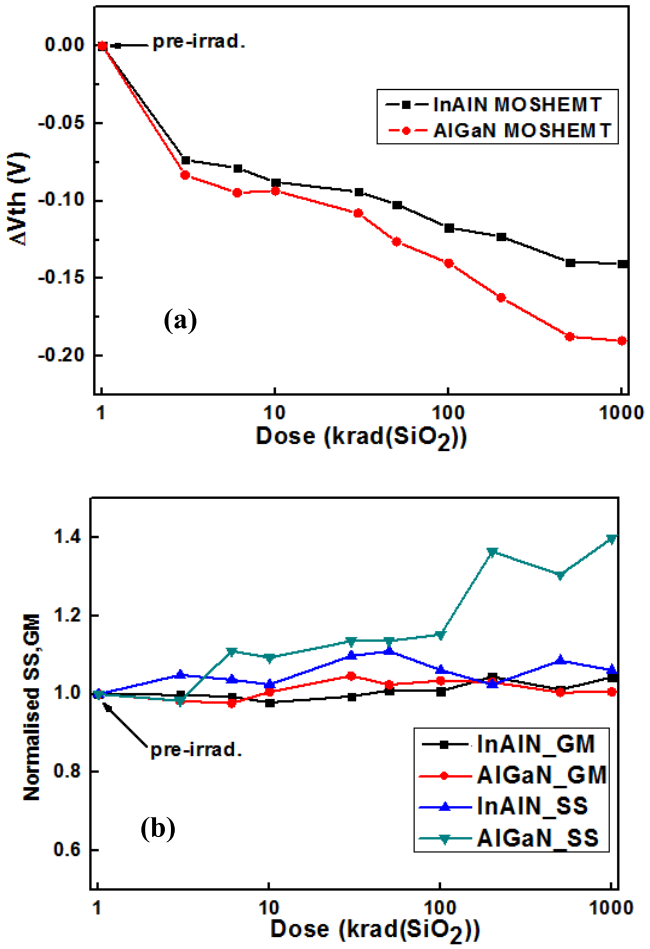

Fig. 6. (a) Threshold voltage shifts. (b) relative changes of G_M and SS for the devices and irradiation conditions of Fig. 5. All terminals are grounded during radiation.

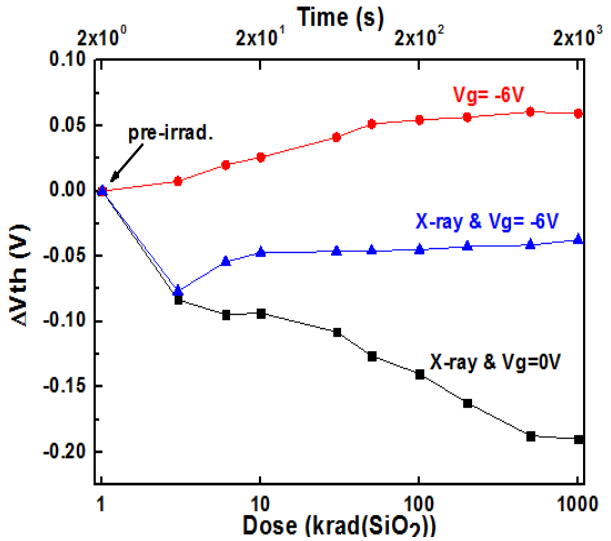

Fig. 7. Effects of negative-bias stress without irradiation (red dots), negative-bias irradiation (blue triangles) and 0-V irradiation on V_{th} shifts of AlGaN MOSHEMTs with 4-nm Al_2O_3 and 8-nm MgCaO as gate dielectric.

The application of negative gate bias ($V_g = -6$ V) leads to a positive V_{th} shift that increases with time [18], as shown in Fig. 7. The positive V_{th} shift for the bias-only case may occur in this case due to electron injection from the gate, which is electrostatically favored under this bias condition. This charge may become trapped in the dielectric layer or neutralize the process-induced positive charge. For irradiation under negative bias, a combination of electron and hole trapping is observed, with net hole trapping dominating over electron trapping in these MOSHEMTs, thus leading to net negative V_{th} shifts for the biased irradiation in Fig. 7. Similar effects are commonly observed in high-K dielectrics [30]. For the 0-V irradiation, radiation-induced-hole trapping is present, but bias-induced electron trapping is not, leading to the most negative V_{th} shift of the three cases shown.

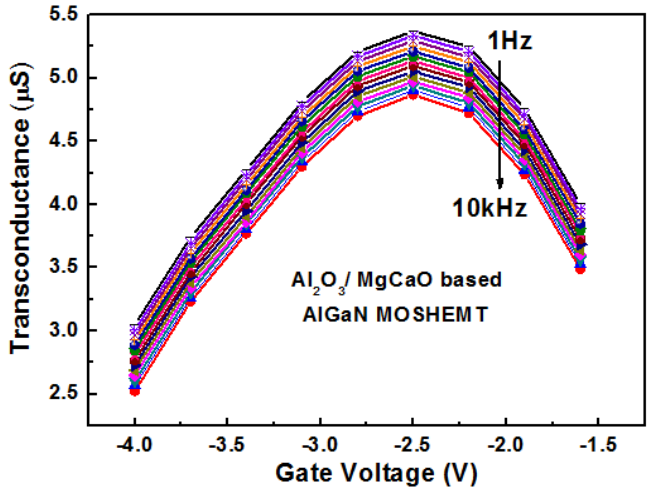

Fig. 8. ACGM measurements of AlGaN/GaN-based MOSHEMTs with 4-nm Al2O3 and 8-nm MgCaO as gate dielectric subjected to bias stress.

D. AC Transconductance Measurements

To provide insight into the source of electron trapping during the bias-only stress, ac transconductance (ACGM) measurements were performed. The measurement set up consists of a lock-in amplifier which produces dc and ac signal with 25-mV amplitude. The signals are superimposed using an ac–dc mixture and is then applied onto the gate of the device. The drain current, obtained with the applied signal, is then fed through a current–voltage converter back into the lock-in amplifier. Subsequently, the lock-in amplifier measures the variation of the drain current (i.e., the fed-back signal) which divided by ac amplitude gives the ACGM [31]. At a fixed gate voltage, ac signals at frequencies ranging from 1 Hz to 10 kHz are superimposed on a fixed gate voltage, and the corresponding values of G_M is recorded as shown in Fig. 8. Frequency dispersion of G_M occurs due to trapping of carriers, provided by the gate metal, by traps existing in different regions of the gate oxide. More details about the ACGM measurement can be found in [31].

The sign of the G_M dispersion with ac signal frequency (i.e., $dG_M/d\ln\,\omega$) also provides information about the trapping mechanism. Decreasing G_M (i.e., negative sign) with increasing frequency suggests electron trapping arising from gate injection, consistent with the bias stress only results in Fig. 7, and as also observed in other gate oxides for MOSHEMTs [31].

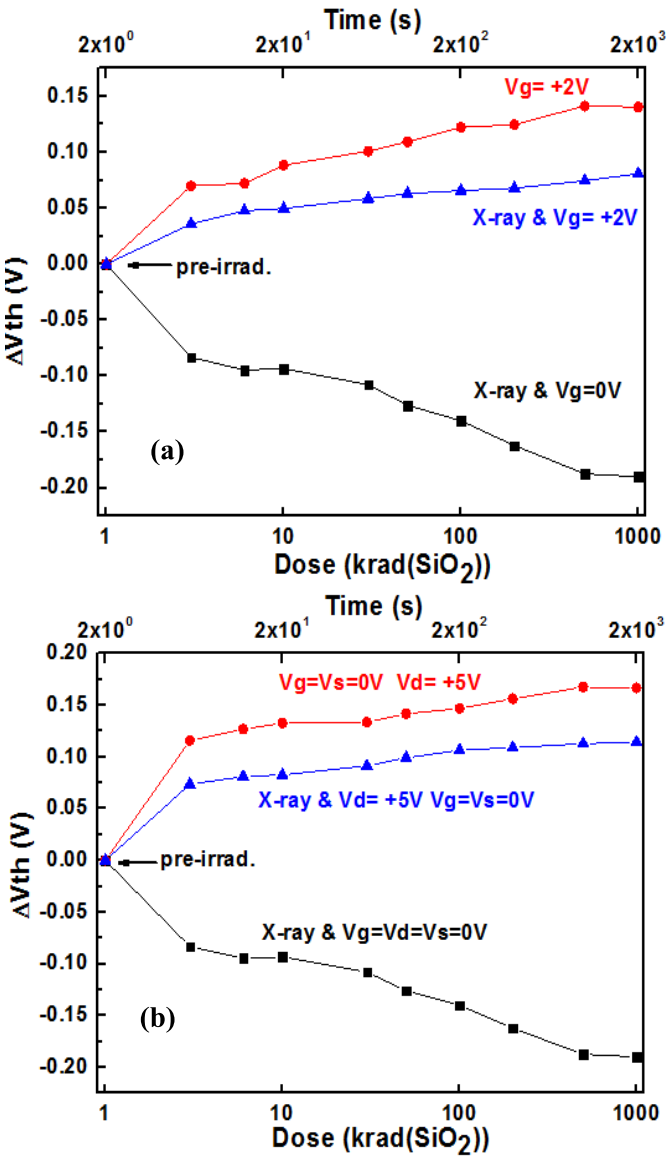

Fig. 9. Effects of (a) gate and (b) drain biases on the bias-stress (red dots), and positive-bias (blue triangles) and 0-V bias (black squares) radiation responses of AlGaN/GaN-based MOSHEMTs with 4-nm Al_2O_3 and 8-nm MgCaO as gate dielectric.

The impact of positive gate (V_g) and drain (V_d) biases on MOSHEMT radiation responses is shown in Fig. 9(a) and (b), respectively. Similar trends are observed to those in Fig. 7, depending on the applied bias. For positive (a) gate or (b) drain bias without irradiation, electron trapping now results from substrate injection, in contrast to the gate injection observed in Fig. 7 under negative gate bias. Radiation-induced holes can neutralize or compensate a fraction of the bias-induced negative charge, reducing the magnitudes of the observed radiation-induced V_{th} shifts in Fig. 9(a) and (b). Similar trends have been observed in studies of combined bias and TID effects in AlGaN/GaN HEMTs [18], [32]. The presence of the dielectric layers in these devices has not led to significantly greater TID degradation than observed in Schottky gate devices of [18], reinforcing the promise of these structures for potential future application in a space environment.

IV. Conclusion

The radiation hardness of GaN HEMTs improves with increasing GaN channel thickness, most likely because of a reduced defect density in as-processed GaN and AlGaN layers. In epitaxial MgCaO-based GaN MOSHEMTs, when grounded, net hole trapping in the oxide gate-stack leads to negative threshold voltage shifts. Electron trapping leads to positive shifts during bias stressing. Both negative and positive shifts are observed during biased irradiation, depending on the bias applied and the relative efficiencies of competing bias-induced electron and radiation-induced-hole-trapping effects in these devices. The results of this paper demonstrate the importance of channel layer thickness to the radiation response of AlGaN/GaN HEMTs, and also show that epitaxial MgCaO is a promising radiation-tolerant gate dielectric material for GaN-based MOSHEMTs.

References

[1] H. Kambayashi *et al.*, "Over 100 A operation normally-off AlGaN/GaN hybrid MOS-HFET on Si substrate with high-breakdown voltage," *Solid-State Electron.*, vol. 54, no. 6, pp. 660–664, Jun. 2010.

[2] R. Chu *et al.*, "1200-V normally off GaN-on-Si field-effect transistors with low dynamic ON-resistance," *IEEE Electron Device Lett.*, vol. 32, no. 5, pp. 632–634, May 2011.

[3] M. Kanamura *et al.*, "Enhancement-mode GaN MIS-HEMTs with n-GaN/i-AlN/n-GaN triple cap layer and high-k gate dielectrics," *IEEE Electron Device Lett.*, vol. 31, no. 3, pp. 189–191, Mar. 2010.

[4] F. Medjdoub *et al.*, "Low on-resistance high-breakdown normally off AlN/GaN/AlGaN DHFET on Si Substrate," *IEEE Electron Device Lett.*, vol. 31, no. 2, pp. 111–113, Feb. 2010.

[5] X. Liu *et al.*, "High voltage AlGaN/GaN metal–oxide–semiconductor high-electron mobility transistors with regrown $In_{0.14}Ga_{0.86}N$ contact using a CMOS compatible gold-free process," *Appl. Phys. Exp.*, vol. 7, no. 12, p. 126501, Dec. 2014.

[6] S. Joglekar, M. Azize, M. Beeler, E. Monroy, and T. Palacios, "Impact of recess etching and surface treatments on ohmic contacts regrown by molecular-beam epitaxy for AlGaN/GaN high electron mobility transistors," *Appl. Phys. Lett.*, vol. 109, no. 4, Jul. 2016, Art. no. 041602.

[7] M. H. S. Owen, M. A. Bhuiyan, Q. Zhou, Z. Zhang, J. S. Pan, and Y.-C. Yeo, "Band alignment of $HfO_2/Al_{0.25}Ga_{0.75}N$ determined by X-ray photoelectron spectroscopy: Effect of SiH_4 surface treatment," *Appl. Phys. Lett.*, vol. 104, no. 9, Mar. 2014, Art. no. 091605.

[8] M. H. S. Owen, M. A. Bhuiyan, Z. Zhang, J. S. Pan, E. S. Tok, and Y.-C. Yeo, "Band alignment of $HfO_2/In_{0.18}Al_{0.82}N$ determined by angle-resolved X-ray photoelectron spectroscopy," *Appl. Phys. Lett.*, vol. 105, no. 3, Jul. 2014, Art. no. 031602.

[9] A. Malmros *et al.*, "Evaluation of thermal versus plasma-assisted ALD Al_2O_3 as passivation for InAlN/AlN/GaN HEMTs," *IEEE Electron Device Lett.*, vol. 36, no. 3, pp. 235–237, Mar. 2015.

[10] D. Xu *et al.*, "0.1-μm atomic layer deposition Al_2O_3 passivated InAlN/GaN high electron-mobility transistors for E-band power amplifiers," *IEEE Electron Device Lett.*, vol. 36, no. 5, pp. 442–444, May 2015.

[11] K.-A. Son *et al.*, "GaN-based high temperature and radiation-hard electronics for harsh environments," *Nanosci. Nanotechnol. Lett*, vol. 2, no. 2, pp. 89–95, 2010.

[12] S.-J. Chang *et al.*, "Dependence of GaN channel thickness on the transistor characteristics of AlGaN/GaN HEMTs grown on sapphire," *ECS J. Solid State Sci. Technol.*, vol. 5, no. 12, pp. N102–N107, 2016.

[13] H. Zhou *et al.*, "High-performance InAlN/GaN MOSHEMTs enabled by atomic layer epitaxy MgCaO as gate dielectric," *IEEE Electron Device Lett.*, vol. 37, no. 5, pp. 556–559, May 2016.

[14] X. Lou *et al.*, "Epitaxial growth of $Mg_xCa_{1-x}O$ on GaN by atomic layer deposition," *Nano Lett.*, vol. 16, pp. 7650–7654, Nov. 2016.

[15] X. Sun *et al.*, "Total-ionizing-dose radiation effects in AlGaN/GaN HEMTs and MOS-HEMTs," *IEEE Trans. Nucl. Sci.*, vol. 60, no. 6, pp. 4074–4079, Dec. 2013.

[16] I. K. Samsel *et al.*, "Charge collection mechanisms in AlGaN/GaN MOS high electron mobility transistors," *IEEE Trans. Nucl. Sci.*, vol. 60, no. 6, pp. 4439–4445, Dec. 2013.

[17] J. Chen *et al.*, "Proton-induced dehydrogenation of defects in AlGaN/GaN HEMTs," *IEEE Trans. Nucl. Sci.*, vol. 60, no. 6, pp. 4080–4086, Dec. 2013.

[18] J. Chen *et al.*, "Effects of applied bias and high field stress on the radiation response of GaN/AlGaN HEMTs," *IEEE Trans. Nucl. Sci.*, vol. 62, no. 6, pp. 2423–2430, Dec. 2015.

[19] R. Jiang *et al.*, "Worst-case bias for proton and 10-keV X-ray irradiation of AlGaN/GaN HEMTs," *IEEE Trans. Nucl. Sci.*, vol. 64, no. 1, pp. 218–225, Jan. 2017.

[20] S.-J. Chang *et al.*, "Investigation of channel mobility in AlGaN/GaN high-electron-mobility transistors," *Jpn. J. Appl. Phys.*, vol. 55, no. 4, Feb. 2016, Art. no. 044104.

[21] S. Ren *et al.*, "Total ionizing dose (TID) effects in GaAs MOSFETs with La-based epitaxial gate dielectrics," *IEEE Trans. Nucl. Sci.*, vol. 64, no. 1, pp. 164–169, Jan. 2017.

[22] F. El Mamouni *et al.*, "Fin-width dependence of ionizing radiation-induced subthreshold-swing degradation in 100-nm-gate-length FinFETs," *IEEE Trans. Nucl. Sci.*, vol. 56, no. 6, pp. 3250–3255, Dec. 2009.

[23] D. M. Fleetwood, "Total ionizing dose effects in MOS and low-dose-rate-sensitive linear-bipolar devices," *IEEE Trans. Nucl. Sci.*, vol. 60, no. 3, pp. 1706–1730, Jun. 2013.

[24] S. Ren *et al.*, "Total ionizing dose (TID) effects in ultra-thin body Ge-on-Insulator (GOI) junctionless CMOSFETs with recessed source/drain and channel," *IEEE Trans. Nucl. Sci.*, vol. 64, no. 1, pp. 176–180, Jan. 2017.

[25] N. S. Saks and M. G. Ancona, "Generation of interface states by ionizing radiation at 80 K measured by charge pumping and subthreshold slope techniques," *IEEE Trans. Nucl. Sci.*, vol. NS-34, no. 6, pp. 1347–1354, Dec. 1987.

[26] J. R. Schwank, D. M. Fleetwood, P. S. Winokur, P. V. Dressendorfer, D. C. Turpin, and D. T. Sanders, "The role of hydrogen in radiation-induced defect formation in polysilicon gate MOS devices," *IEEE Trans. Nucl. Sci.*, vol. NS-34, no. 6, pp. 1152–1158, Dec. 1987.

[27] R. K. Freitag, E. A. Burke, C. M. Dozier, and D. B. Brown, "The development of non-uniform deposition of holes in gate oxides," *IEEE Trans. Nucl. Sci.*, vol. NS-35, no. 6, pp. 1203–1207, Dec. 1988.

[28] D. M. Fleetwood *et al.*, "Oxygen-related border traps in MOS and GaN devices," in *Proc. IEEE Int. Conf. Solid-State Integr. Circuit Technol.*, Xi'an, China, Oct./Nov. 2012, pp. 1–4.

[29] S. Liu *et al.*, "Interface/border trap characterization of Al_2O_3/AlN/GaN metal–oxide–semiconductor structures with an AlN interfacial layer," *Appl. Phys. Lett.*, vol. 106, no. 5, Feb. 2015, Art. no. 051605.

[30] G. X. Duan *et al.*, "Bias dependence of total ionizing dose effects in SiGe-MOS FinFETs," *IEEE Trans. Nucl. Sci.*, vol. 61, no. 6, pp. 2834–2838, Dec. 2014.

[31] X. Sun *et al.*, "Study of gate oxide traps in HfO_2/AlGaN/GaN metal–oxide–semiconductor high-electron-mobility transistors by use of AC transconductance method," *Appl. Phys. Lett.*, vol. 102, no. 10, Mar. 2013, Art. no. 103504.

[32] J. Chen *et al.*, "High-field stress, low-frequency noise, and long-term reliability of AlGaN/GaN HEMTs," *IEEE Trans. Device Mater. Rel.*, vol. 16, no. 3, pp. 282–289, Sep. 2016.